

A Cylindrical Galton Board at the Galton Board's 150th Anniversary

Kanti V. Mardia ¹, Colin Goodall ¹ and John Rubbo ²

¹ k.v.mardia@leeds.ac.uk; colin.goodall1@gmail.com; University of Leeds, Leeds LS2 9JT, UK

² jrubbo48@aol.com; Little Brown House, Matawan NJ, USA

Abstract

The celebrated Galton board remains a widely used device for demonstrating how repeated Bernoulli trials on a triangular lattice generate an approximately normal distribution. Marking the 150th anniversary of Galton's 1875 construction, this paper revisits the historical apparatus and extends it to a cylindrical setting in which the peg lattice is wrapped around a cylinder, enforcing angular periodicity and producing height-dependent behaviour absent from the classical design. This modification connects Galton's original demonstration of variation and the emergence of the normal distribution with modern developments in circular statistics, providing a physical realisation of binomial random walks on a circular-linear product space. We distinguish configurations where the wrapped lattice subtends only a strict arc from those spanning the full circumference, and show how the resulting geometry yields wrapped binomial and wrapped normal behaviour. We describe the design and construction of our physical model, outline practical considerations for replication, and analyse the statistical properties and pedagogical applications of this cylindrical variant, which offers a modern reinterpretation of Galton's pioneering work.

Keywords: binomial distribution, Galton board construction, directional statistics, physical cylindrical board, wrapped binomial distribution, wrapped normal distribution

1 Introduction

Modern implementations of the celebrated Galton board continue to be widely used. For example, the STEM Galton Board produced by Index Fund Advisors (IFA) has

sold more than 60,000 units worldwide and is accompanied by extensive instructional material, videos, and a detailed user guide linking the device to random behaviour in financial markets. This contemporary version is described at <https://www.ifa.com/galtonboard>.

The enduring popularity of such devices reflects the continuing pedagogical value of physical demonstrations of probabilistic variation

The classical planar Galton board provides a vivid illustration of how a normal distribution emerges from repeated independent binary decisions. Balls traverse a triangular array of pegs and accumulate in bins at the base, but the planar geometry necessarily introduces artificial lateral boundaries that break translational symmetry and influence the resulting distribution. These geometric constraints are rarely discussed but have important implications for the interpretation of the device.

In this paper, we propose a cylindrical Galton board obtained by wrapping the peg lattice continuously around a solid cylinder. This construction enforces periodic boundary conditions in the horizontal direction and yields a natural circular bin structure. The resulting device provides a physical realisation of a binomial random walk on the manifold $S^1 \times \mathbb{R}$, leading naturally to the wrapped normal distribution. The cylindrical geometry restores horizontal symmetry, eliminates boundary effects, and offers a new perspective on Galton’s original pedagogical aims.

The remainder of the paper is organised as follows. Section 2 summarises the historical development of the Galton board and its role in nineteenth-century statistical thought. Section 3 presents a detailed parametrisation of a Galton board whose peg lattice is embedded on the surface of a solid cylinder. Section 4 describes the underlying wrapped distributions, including the wrapped binomial and the wrapped normal. Section 5 discusses stochastic dynamics on the cylindrical board. Section 6 reports on the construction of our physical cylindrical board and its operation. Section 7 concludes with a discussion. Appendix A constructs a cylindrical model by wrapping a synthetic Galton board.

2 Historical Context

Francis Galton’s probability machine, later known as the Galton board or *quincunx*, occupies a distinctive place in the development of nineteenth-century statistical thought. Although the device is now familiar from modern demonstrations of the central limit theorem, its origins lie in Galton’s broader programme of illustrating variation, error, and regression through physical apparatus.

Galton first alluded to the mechanism in his 1875 paper (Galton, 1875), where he used a peg-based device to demonstrate regression to the mean and the emergence of the normal distribution. A fuller description appeared in Galton (1877), and an extended treatment was later included in his 1889 book (Galton, 1889, pp. 63–70),

Natural Inheritance. In these works, the board served not merely as a curiosity but as a concrete embodiment of the binomial law of error, illustrating how aggregate regularity arises from individual randomness.

The apparatus also featured prominently in Galton's public lectures, including his Royal Society demonstrations, where it provided a striking visualisation of the central limit phenomenon. Stigler's historical analysis (Stigler, 1986, pp. 275–281) situates the device within the broader nineteenth-century effort to communicate probabilistic ideas to scientific and lay audiences alike. The quincunx exemplified Galton's belief that statistical principles could be made accessible through carefully designed physical models.

Digital versions of the Galton board are now widely available, including interactive apps and online simulations that allow users to vary the number of rows, probabilities, and visual settings. These modern implementations continue Galton's original aim of making probabilistic ideas accessible to broad audiences, and illustrate the enduring pedagogical appeal of the device.

For completeness, readers may wish to view a demonstration of Galton's original 1873 apparatus, which can be seen in operation during the first two minutes of the following video:

<https://www.youtube.com/watch?v=SZoDNfVFS7I>.

These historical materials highlight the pedagogical and conceptual motivations behind the device and provide context for our cylindrical extension, which seeks to preserve Galton's original aims while addressing geometric limitations inherent in the planar design.

3 Cylindrical Geometry and Peg Lattice

We introduce here the geometric and lattice parameters required for a cylindrical Galton board. A right circular cylinder of radius R is parameterised by angular coordinate $\theta \in [0, 2\pi)$ and vertical coordinate $z \in \mathbb{R}$, as illustrated in Figure 1. The circumference is $C = 2\pi R$.

We consider peg lattices on the cylinder where adjacent pegs on the same row are separated by horizontal arc length $d > 0$, and successive rows are separated vertically by $h > 0$. The angular spacing between neighbouring pegs is therefore

$$\Delta\theta = \frac{d}{R},$$

and we choose d (equivalently $\Delta\theta$) so that the circle is divided into an integer number M of angular slots:

$$M = \frac{C}{d} = \frac{2\pi}{\Delta\theta}.$$

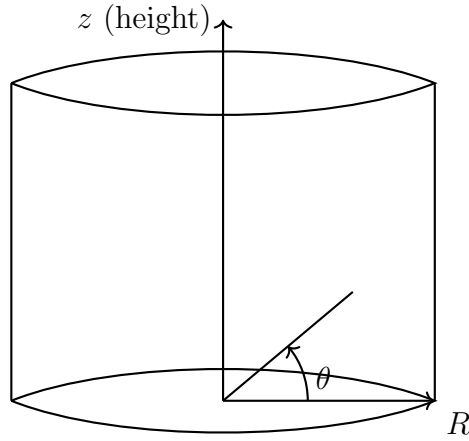


Figure 1: Cylindrical Galton board with labelled axes: drops evolve vertically (z direction), collisions rotate angular position (θ), and bins wrap around the circular base.

Rows are indexed by $i = 0, 1, \dots, n$. Row i contains $i + 1$ pegs in the unwrapped triangular lattice and

$$i_M = \min(M, i + 1)$$

pegs when wrapped onto the cylinder. Table 1 summarises the geometric and lattice parameters.

Table 1: Summary of cylindrical Galton board parameters

Parameter	Description
M	Number of angular bins
$\Delta\theta$	Angular spacing between pegs (bin width)
d	Horizontal arc length between adjacent pegs
h	Vertical spacing between rows of pegs
n	Number of peg rows
H	Total cylinder height
R	Cylinder radius
C	Circumference, $C = 2\pi R$
r_p	Peg radius
r_b	Ball radius
H_{module}	Module height (e.g. $8h$ for 8 peg rows)
H_{bin}	Bin height (e.g. $2H_{\text{module}}$)

The angular and vertical coordinates of the pegs are

$$\theta_{i,j} = \left(j - \frac{i}{2}\right) \Delta\theta \pmod{2\pi}, \quad z_i = H - ih,$$

for $j = 0, 1, \dots, i_M - 1$ and $i = 0, 1, \dots, n - 1$. The corresponding Cartesian coordinates are

$$x_{i,j} = R \cos \theta_{i,j}, \quad y_{i,j} = R \sin \theta_{i,j}, \quad z_{i,j} = z_i.$$

An illustrative unwrapped representation of the peg lattice, showing the row index i and column index j , is given in Figure 2.

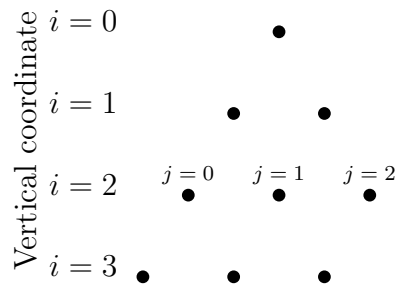


Figure 2: Illustrative peg lattice showing row index i and column index j for the angular coordinate $\theta_{i,j}$.



Figure 3: Front view of the cylindrical Galton board obtained by wrapping a synthetic planar Galton board. Further details are provided in Appendix A .

Figure 3 shows a front view of the cylindrical Galton board, illustrating the perspective obtained after wrapping a synthetic planar model.

4 Wrapped Binomial and Wrapped Normal Distributions

4.1 Wrapped binomial distribution

We follow Section 3.5.7 of Mardia and Jupp (2000) in introducing wrapped distributions. Let $X \sim \text{Bin}(n, p)$ with support $\{0, 1, \dots, n\}$, and let $M \geq 1$ be an integer. The *wrapped binomial distribution* on the finite cyclic group $\mathbb{Z}_M = \{0, 1, \dots, M-1\}$ is defined by

$$Y = X \bmod M.$$

For $k \in \mathbb{Z}_M$, the probability mass function is

$$\Pr(Y = k) = \sum_{\ell \geq 0: k + \ell M \leq n} \binom{n}{k + \ell M} p^{k + \ell M} (1 - p)^{n - k - \ell M}. \quad (4.1)$$

The characteristic function of the wrapped binomial is

$$\phi_\theta(t) = \mathbb{E}[e^{it\Theta}] = (1 - p + p e^{it2\pi/M})^n.$$

For $p = 1/2$, this simplifies to

$$\phi_\theta(t) = \left(\cos \frac{\pi t n}{M} \right)^n \exp\left(\frac{i \pi t n}{M} \right), \quad (4.2)$$

and the first trigonometric moments are

$$\alpha_1 = \cos^2\left(\frac{\pi n}{M}\right), \quad \beta_1 = \cos\left(\frac{\pi n}{M}\right) \sin\left(\frac{\pi n}{M}\right).$$

Hence the resultant length ρ and mean direction μ are

$$\rho = \left| \cos \frac{\pi n}{M} \right|, \quad \mu = \frac{\pi n}{M}. \quad (4.3)$$

As $M \rightarrow \infty$ for fixed n , we have $\rho \rightarrow 1$, showing that the wrapped binomial becomes highly concentrated at zero mean. If instead $M \rightarrow \infty$ and $n \rightarrow \infty$ with $\delta = n/M$ fixed, then from (4.2) the characteristic function tends to that of the uniform distribution on \mathbb{Z}_M , since $|\cos(\pi t n/M)| < 1$ while $\exp(i \pi t n/M) = \exp(i \pi t \delta)$ remains fixed.

For the wrapped binomial (4.1), we compute probabilities for various values of n with $M = 24$; this choice of M corresponds to our physical model in Section 6. Figure 4 shows that $n \geq 24$ is required for full support on $(-\pi, \pi]$, and that the distribution approaches the discrete uniform as n increases.

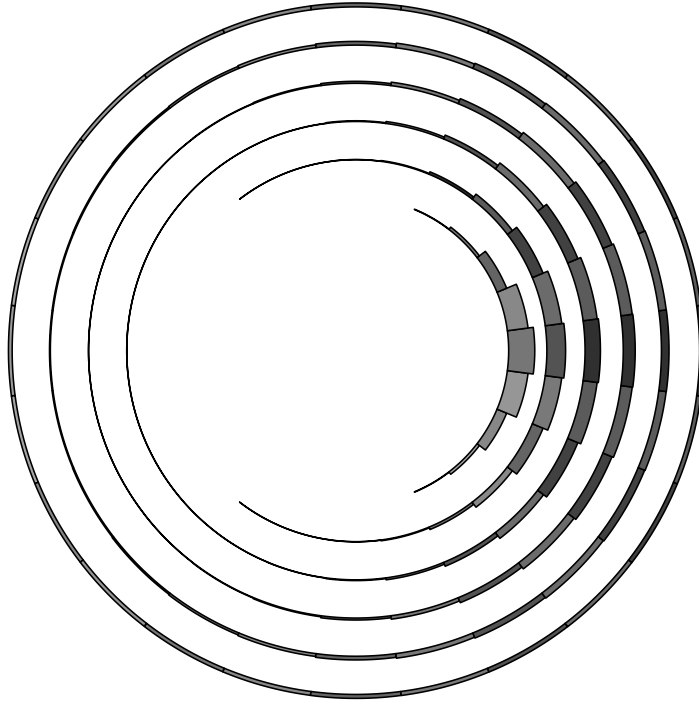


Figure 4: Concentric curved barplots of wrapped binomial probabilities for $M = 24$ and $n = 8, 16, 24, 40, 100, 400$. The height of each bar is measured from the corresponding circle. The support is strictly smaller than $(-\pi, \pi]$ for small n , and the wrapped binomial approaches the discrete uniform distribution for large n .

4.2 Wrapped normal distribution

The wrapped normal distribution $\text{WN}(\mu, \sigma^2)$ is defined by wrapping a normal random variable $X \sim N(\mu, \sigma^2)$ onto the circle:

$$\Theta = X \bmod 2\pi.$$

Its probability density function on $[0, 2\pi)$ is

$$f_{\text{WN}}(\theta \mid \mu, \sigma^2) = \frac{1}{\sqrt{2\pi\sigma^2}} \sum_{k=-\infty}^{\infty} \exp\left(-\frac{(\theta - \mu + 2\pi k)^2}{2\sigma^2}\right). \quad (4.4)$$

Figure 5 illustrates a wrapped normal distribution plotted on the interior surface of a vertical cylinder of unit radius. The angular coordinate $\theta \in [0, 2\pi)$ determines the horizontal position $(\cos \theta, \sin \theta)$, while the vertical axis represents the radial height of the density.

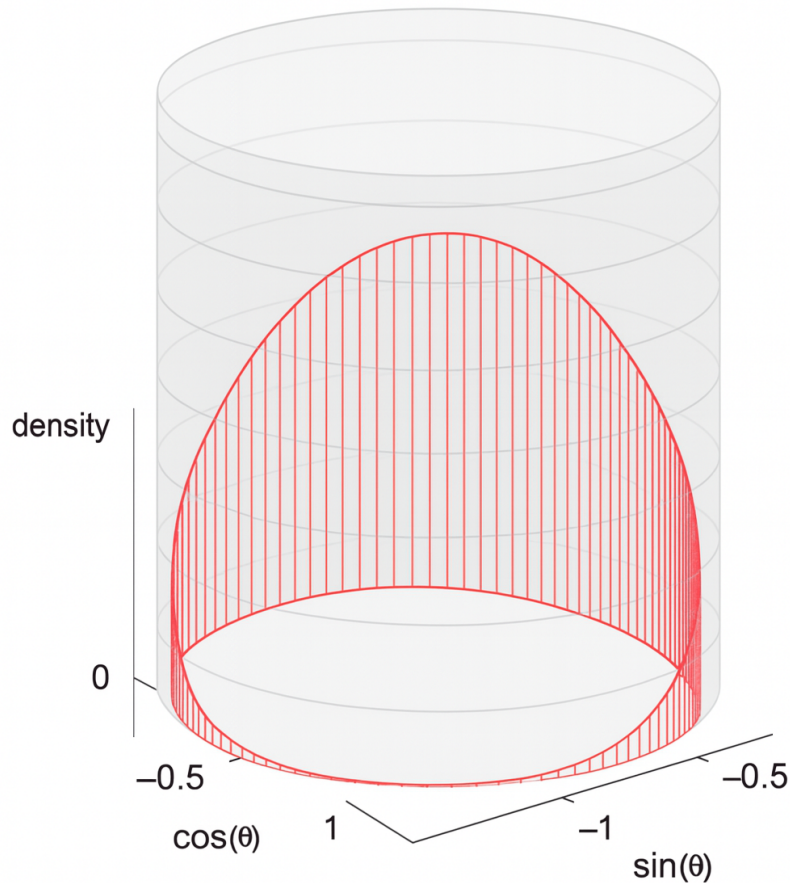


Figure 5: Wrapped normal distribution plotted on the surface of a unit cylinder. For angular coordinate $\theta \in [0, 2\pi)$, the horizontal position is $(\cos \theta, \sin \theta)$, while the vertical axis represents the height $f_{\text{WN}}(\theta)$. The density is shown for $\mu = 0$ and scale parameter σ . Vertical line segments indicate the height above the base circle, forming a smooth crown-like surface.

Figures 3, 4 and 5 together illustrate how geometry transforms the limiting form of distributions. On the planar domain \mathbb{R} , horizontal displacement follows a standard normal

law; when wrapped onto \mathbb{S}^1 , this becomes a wrapped normal; and when implemented physically on a cylindrical surface, the apparatus enforces periodic boundary conditions.

The limiting Gaussian form on \mathbb{R} is consistent with classical pin-board constructions and central limit behaviour (Galton, 1889; Kendall, 1948). Since the planar Gaussian lives on \mathbb{R} and the cylindrical surface lives on $\mathbb{R}/2\pi\mathbb{Z}$, projection to the periodic space induces wrapping (Mardia and Jupp, 2000), confirming the theoretical convergence.

Unimodality and the mode. The wrapped normal distribution is unimodal with its unique mode at the mean direction μ . Although this fact is well known, a concise proof is not easily accessible, so we include one here. From the Fourier series representation (Mardia and Jupp, 2000, p. 50),

$$f(\theta) = \frac{1}{2\pi} \left(1 + 2 \sum_{n=1}^{\infty} e^{-n^2\sigma^2/2} \cos(n(\theta - \mu)) \right),$$

each coefficient $e^{-n^2\sigma^2/2}$ is positive for $n \geq 1$. For fixed n , the term $\cos(n(\theta - \mu))$ attains its maximum value 1 at $\theta = \mu \pmod{2\pi}$ and is strictly smaller elsewhere. Since every term in the series is maximised at $\theta = \mu$, the entire sum is maximised at $\theta = \mu$. Uniqueness follows because at any other θ at least one cosine term is strictly smaller than 1. Hence the wrapped normal has a single global maximum at μ and is unimodal.

5 Stochastic Dynamics on the Cylindrical Board

Given the geometric construction above, we now formalise the stochastic dynamics of a ball descending through the cylindrical peg lattice and characterise the resulting angular distribution at the bins.

5.1 Ball dynamics

Let (Θ_k, Z_k) denote the angular and vertical position of a ball after the k -th deflection, with $(\Theta_0, Z_0) = (0, 0)$. At each row the ball undergoes a binary angular deflection,

$$\Theta_{k+1} = \left(\Theta_k + \xi_k \frac{\Delta\theta}{2} \right) \pmod{2\pi}, \quad Z_{k+1} = Z_k - h,$$

where

$$\xi_k = \begin{cases} +1, & \text{with probability } p, \\ -1, & \text{with probability } 1 - p, \end{cases} \quad k = 1, \dots, n.$$

Thus the ball performs a *helical random walk* on the cylindrical surface. Writing

$$S_n = \sum_{k=1}^n \xi_k, \quad \Theta_n = \left(S_n \frac{\Delta\theta}{2} \right) \pmod{2\pi},$$

the distribution of S_n is binomial,

$$\mathbb{P}(S_n = 2k - n) = \binom{n}{k} p^k (1-p)^{n-k}, \quad k = 0, \dots, n.$$

The base of the cylindrical board is partitioned into M angular slots,

$$C_M: \quad \theta_s = s\Delta\theta \pmod{2\pi}, \quad s = 0, \dots, M-1,$$

with $\Delta\theta = 2\pi/M$. The induced distribution on C_M is precisely the *wrapped binomial distribution* introduced in Section 4.

5.2 Moments, drift, and asymptotics

The mean and variance of the unwrapped angular displacement are

$$\mathbb{E}[\Theta_n] = n(2p-1)\frac{\Delta\theta}{2}, \quad \text{Var}(\Theta_n) = np(1-p)\Delta\theta^2.$$

A bias $p \neq \frac{1}{2}$ produces a systematic rotational drift.

For fixed M , as $n \rightarrow \infty$ the wrapped binomial distribution converges to the discrete uniform distribution on C_M . This behaviour is observed both computationally and physically: once $n > M$, balls routinely traverse past the antipode.

For the joint limit $n \rightarrow \infty$ and $M \rightarrow \infty$ with $n/M \rightarrow \infty$, the unwrapped displacement satisfies the classical central limit theorem,

$$S_n \frac{\Delta\theta}{2} \xrightarrow{d} \mathcal{N}\left(n(2p-1)\frac{\Delta\theta}{2}, np(1-p)\Delta\theta^2\right),$$

and wrapping modulo 2π yields the *wrapped normal limit*

$$\Theta_n \xrightarrow{d} \mathcal{WN}\left(\mu = n(2p-1)\frac{\Delta\theta}{2}, \sigma^2 = np(1-p)\Delta\theta^2\right).$$

If, for illustration, $n = M^\alpha$ with $\alpha > 1$, the wrapped binomial converges simultaneously to the wrapped normal and to the uniform distribution, so the wrapped normal limit is uniform. Conversely, when $n = M$ there is no wrapping.

5.3 Connection to bins

The bins partition the circle into intervals

$$I_k = \left[\frac{2\pi(k-1)}{M}, \frac{2\pi k}{M} \right), \quad k = 1, \dots, M.$$

The probability of landing in bin k is

$$p_k = \int_{I_k} f_{\text{WN}}(\theta) d\theta,$$

where f_{WN} is the wrapped normal density from the asymptotic result above. This discrete distribution constitutes the observable output of the cylindrical Galton board.

5.4 Unified framework

The transition kernel for the angular walk has the form

$$p_{n+1}(x) = p p_n(x - 1) + q p_n(x + 1),$$

mirroring the classical planar Galton board but on the compact group C_M or S^1 . This identifies the wrapped normal as the natural circular analogue of the Gaussian limit, consistent with general theory on random walks on compact groups and circular statistics (Dhungana and Fragoso, 2016; Kato, 2010; Mardia and Jupp, 2000; Su, 1998).

For comparison, the planar Galton board produces horizontal displacements

$$X_n = 2(X - np) = \sum_{i=1}^n S_i, \quad S_i \in \{-1, +1\},$$

with

$$X_n \Rightarrow \mathcal{N}((p - q)n, 4npq),$$

giving rise to the familiar near-normal distribution observed at the base of the classical device. For the symmetrical case, $X_n \Rightarrow \mathcal{N}(0, n)$.

6 Physical Cylindrical Model

We have constructed a physical cylindrical Galton board comprising four main components:

- Funnel** A ball hopper and funnel at the top, containing approximately 1000 small steel ball bearings.
- Modules** Five modules, each with 8 rows of pegs. Each row contains up to $M = 24$ pegs with constant angular spacing $\Delta\theta = 2\pi/24 = 15^\circ$. Modules 1–3 contain the triangular peg lattice, while modules 4–5 contain a rectangular lattice; all rows are staggered.
- Bins** A set of $M = 24$ equally spaced collection bins arranged around the base of the cylinder.
- Frame** A reset mechanism that returns balls from the collection bins to the hopper by rotating the apparatus.

When balls are dropped, the angular distribution after n rows of pegs corresponds to a wrapped binomial distribution $WB(n, M)$, approximating a wrapped normal (WN) distribution. Each additional row of pegs allows a ball to travel an additional angular displacement of $\Delta\theta/2 = 7.5^\circ$ beyond the antipode; we refer to this as “wrapping to”.

Table 2: Discrete angular distributions for the five-module physical model

Modules	Distribution
1	Binomial with $n = 8$, approximating WN on $[-60^\circ, +60^\circ]$
1–2	Binomial with $n = 16$, approximating WN on $[-120^\circ, +120^\circ]$
1–3	$WB(24, 24)$, approximating WN with full support $(-180^\circ, 180^\circ]$
1–4	$WB(32, 24)$, approximating WN, wrapping to $(-180^\circ, -120^\circ]$ and $[120^\circ, 180^\circ]$
1–5	$WB(40, 24)$, approximating WN, wrapping to $(-180^\circ, -60^\circ]$ and $[60^\circ, 180^\circ]$

Each module is embedded on the surface of a right circular cylinder of radius 11.5 cm (4.5 in) and height 8.3 cm (3.25 in), containing 8 rows of pegs. Thus the peg field height ranges from 8.3 cm (one module, 8 rows) to 41.5 cm (five modules, 40 rows), and can be extended further by adding additional modules.

The i th row of pegs ($i = 1, \dots, n = 40$) contains $\min(i, 24)$ pegs. Modules 1–3 contain triangular arrangements of 1–8, 9–16, and 17–24 pegs respectively. Modules 4–5, and any subsequent modules, each contain $M = 24$ pegs per row. Pegs in each row are centred on the 0° midline, and successive rows are staggered by $\Delta\theta/2 = 7.5^\circ$, following the classical Galton board geometry. The five modules together contain 684 pegs: 300 in the triangular region (modules 1–3) and 384 in the rectangular region (modules 4–5).

The parameters of the physical model (Table 3) were chosen to ensure that (i) balls fall one at a time through the peg field without interacting, (ii) each ball strikes exactly one peg per row, (iii) balls do not deflect beyond the sides of the peg field, ensured by buffers in the first three modules, and (iv) the five physical configurations correspond to five wrapped binomial distributions, 2, and five different concentration parameters of the wrapped normal limit.

A further consideration is that the balls should follow the cylindrical surface, or more precisely remain within a cylindrical annulus. Pegs extend 6 mm (0.25 in) radially and balls have diameter 4 mm (0.157 in). The apparatus is enclosed in a clear plastic cylinder of internal diameter 12.7 cm (5 in) and wall thickness 6 mm (0.25 in). When the collection bins are arranged around the same 4.5 in internal cylinder, the balls stack in a single layer, typically in a 3–2–3–2 pattern, so that the relative heights of the balls in the bins form a histogram approximating the wrapped binomial distribution and the discretised wrapped normal density.

The number of modules can be increased arbitrarily by extending the height of the containing cylinder. With six modules ($n = 48$ rows), the wrapped binomial distribution covers the circle C_{24} exactly twice. Table 4 extends Table 2 to additional modules Note that the division of rows into modules of eight is a constructional convenience rather

Table 3: Parameters of the physical cylindrical Galton board

Symbol	Description	Count	Value (cm)	Value (in)
H	Total board height (5 modules)		61	24
H_p	Peg field height (5 modules)		41.5	16.25
W	Peg insertion board diameter		11.4	4.5
W^*	Outer cylinder inner diameter		12.7	5
n	Number of peg rows (5 modules)	40		
d	Horizontal peg spacing		1.5	0.589
h	Vertical peg spacing		1.02	0.4
r_{peg}	Peg radius		0.1	0.04
r_{ball}	Ball radius		0.4	0.157
N	Number of balls	1000		
M	Number of bins	24		
b	Bin width		1.4	0.549
H_b	Bin height		13	5.1

than an intrinsic feature of the cylindrical quincunx.

Table 4: Further discrete angular distributions for extended models

Modules	Distribution
1–3	WB(24, 24), approx WN with full support $(-180^\circ, 180^\circ]$
1–6	WB(48, 24), approx WN, wrapping once around the circle
1–9	WB(72, 24), approx WN, wrapping twice around the circle
1–12	WB(96, 24), approx WN, wrapping three times around the circle

The classical planar Galton board yields a normal distribution via the central limit theorem. When wrapped onto a cylinder, the Galton board induces a random walk on $\mathbb{Z} \times S^1$, producing wrapped binomial and wrapped normal laws governed by circular statistics.

Figure 6 presents several views of our physical cylindrical Galton board. The two photographs of the apparatus on the left shows Modules 1–5 together with the collection bins, before the balls have been passed through the peg lattice. The two views on the right show the distribution of 2000 balls in the collection bins, the front view displays the modal region of the resulting approximate wrapped normal distribution, and the lower view shows, at the back of the device, the the tail region of the distribution, including the impact of wrapping. These views demonstrate that the physical model generates an angular distribution that closely approximates the wrapped normal law.

7 Discussion

The cylindrical Galton board introduced here removes the edge effects inherent in planar designs and provides a natural physical realisation of a binomial random walk with

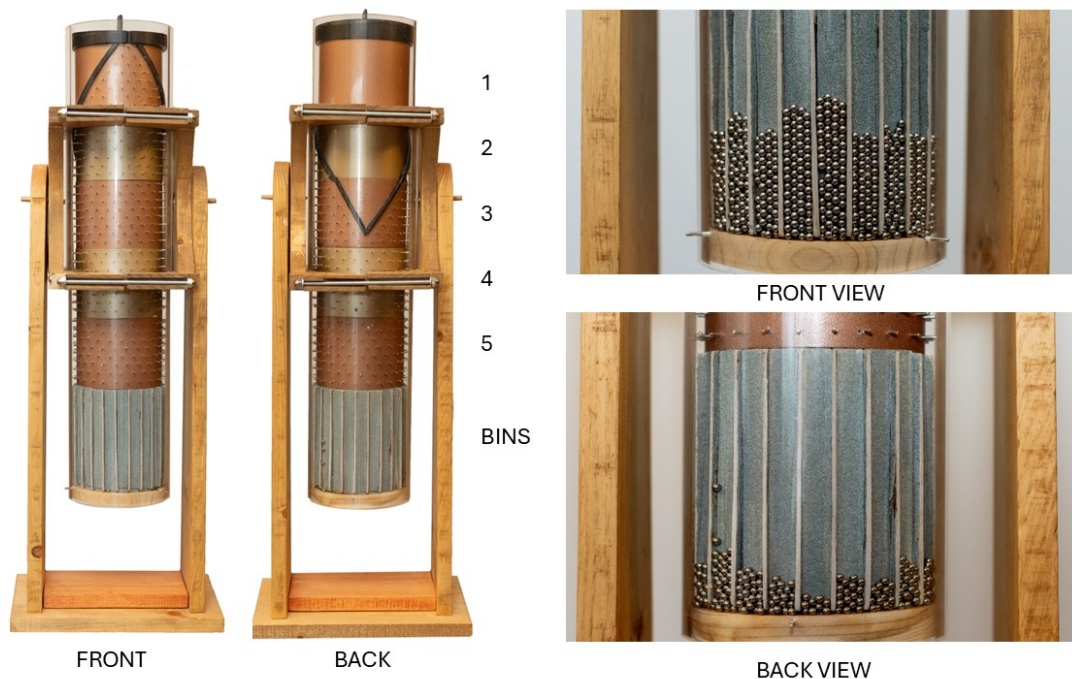


Figure 6: Our physical model; left: The model showing full front and back view with Modules 1-5 and the Bins; right: distribution of 2000 balls in the bins, front view (top) and back view (lower).

periodic boundary conditions. By enforcing angular periodicity, the device transforms the classical left–right deflection process into a random walk on the compact manifold S^1 , thereby linking a familiar nineteenth-century apparatus to modern developments in circular statistics and stochastic processes on manifolds.

The geometry of the device plays a decisive role in shaping the resulting distributional behaviour. On the planar board, the horizontal displacement evolves on an unbounded linear domain and the classical Central Limit Theorem yields a Gaussian limit. On the cylindrical board, the same local dynamics unfold on a compact domain, producing wrapped binomial and wrapped normal laws and, for fixed M , eventual convergence to the discrete uniform distribution. This contrast highlights a broader principle: the topology of the state space determines the global behaviour of the random walk, even when the local transition mechanism is unchanged. The cylindrical board therefore provides a rare physical demonstration of how geometric constraints and boundary conditions influence probabilistic limits.

From a pedagogical perspective, the cylindrical Galton board offers several advantages. It provides a tangible illustration of periodic boundary conditions, a concept that is central in fields ranging from statistical physics to computational modelling. It also offers a concrete demonstration of wrapped distributions, which are typically introduced abstractly in courses on directional statistics. The modular construction allows instructors to vary the number of rows and bins, enabling students to observe directly the transition from binomial to wrapped normal to uniform behaviour. This flexibility

makes the device a valuable teaching tool for illustrating the interplay between geometry, randomness, and limiting distributions.

The physical model also has methodological value. Because the device can be extended by adding modules, it provides a controlled environment for studying how the parameters n and M influence the emergence of wrapped distributions. This makes it suitable for simulation studies in which symmetry, invariance, and boundary behaviour are of interest. The cylindrical board can serve as a physical analogue for random walks on compact groups, offering an experimental platform for validating theoretical results in circular statistics, stochastic processes, and harmonic analysis on S^1 .

Beyond its immediate applications, the cylindrical Galton board suggests several avenues for further investigation. One direction concerns the behaviour of biased walks, where the interaction between drift and periodicity leads to non-trivial stationary distributions. Another concerns the extension to higher-dimensional manifolds, such as random walks on tori or spheres, where physical analogues may be constructed by embedding peg lattices on curved surfaces. A third direction involves further study of mixing times and rates of convergence to the wrapped normal or uniform distributions, which may depend sensitively on the ratio n/M and on the geometry of the peg lattice.

Finally, the cylindrical Galton board offers a modern reinterpretation of Galton's original device. Whereas Galton used the planar board to illustrate regression, variation, and the emergence of the normal distribution, the cylindrical version extends these ideas to the circular setting, connecting classical probability demonstrations with contemporary statistical theory. In doing so, it provides a bridge between historical intuition and modern geometric perspectives, illustrating how simple physical constructions can illuminate deep probabilistic principles.

8 Acknowledgments

We wish to thank John Kent for his helpful comments.

References

- Dhungana, J. and Fragoso, M. D. (2016) Random walks on finite cyclic groups. *Stochastic Processes and their Applications*, **126**, 3714–3732.
- Galton, F. (1875) Statistics by intercomparison, with remarks on the law of frequency of error. *Philosophical Magazine, 4th series*, **49**, 33–46.
- (1877) Typical laws of heredity. *Proceedings of The Royal Institution of Great Britain*, **8**, 282–301.
- (1889) *Natural Inheritance*. London: Macmillan.

- Kato, S. (2010) A markov process for circular data. *Journal of the Royal Statistical Society: Series B*, **72**, 655–672.
- Kendall, M. G. (1948) On the generalized “binomial” distribution. *Biometrika*, **35**, 28–44.
- Mardia, K. V. and Jupp, P. E. (2000) *Directional Statistics*. Wiley.
- Stigler, S. M. (1986) *The History of Statistics: The Measurement of Uncertainty Before 1900*. Belknap Press of Harvard University Press.
- Su, F. E. (1998) Convergence of random walks on the circle generated by an irrational rotation. *Transactions of the American Mathematical Society*, **350**, 3717–3741.

A Appendix: Synthetic Cylindrical Galton Board

We now construct a synthetic planar Galton board which then wrapped onto a cylinder to create a cylindrical Galton board. The board consists of $n = 10$ rows of pegs with horizontal spacing $d = 1$ cm and vertical spacing $h = 0.8$ cm. Balls again undergo independent left–right deflections with probability $p = 0.5$ at each peg, resulting in $M = n + 1 = 11$ collection bins at the base. The side walls are inclined at angle $\theta = 30^\circ$. The resulting bin counts approximate a binomial distribution and, for large n , a normal distribution as seen in Figure 7.

Wrapping the Synthetic Board. We now wrap our synthetic Galton Board in Figure 7. The frontal view of the wrapped cylindrical Galton board given in Figure 3 shows the funnel, the full triangular lattice of $n = 11$ peg rows, and the visible subset of collection bins at the base. The device is obtained by wrapping the short side (210 mm) of a planar A4 Galton board, with $n = 11$ peg rows and $m = 11$ bins, around a cylinder of radius $r \approx 33.4$ mm and height 297 mm. In this projection, only the central portion of the circular bin ring is visible, so the bins are labeled from 3 to 9, corresponding to a contiguous subset of the full sequence of 11 bins. The bell-shaped accumulation of balls in these bins reflects the approximately wrapped normal distribution generated by the random left–right deflections at each peg, while the curvature of the cylindrical casing makes clear that additional bins exist beyond the visible window.

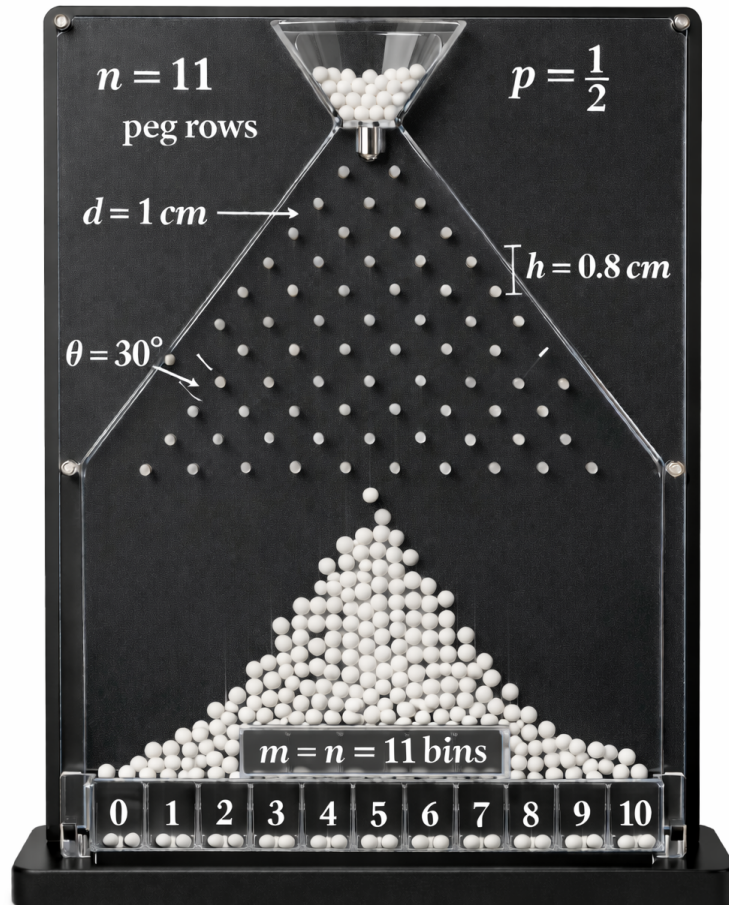


Figure 7: A synthetic Galton Board Classic planar Galton board Board size= A4 size. m =number of bins here and n = number of rows.



Front View

Figure 8: Wrapping the synthetic Galton Board Figure 7. The Front view of the cylindrical Galton board formed by wrapping the short side of this planar A4 board. Reproduced in the Paper.